# Energy levels and intersubband transitions in InGaAsN/AlGaAs quantum wells

Jean-Yves Duboz*
*CRHEA, CNRS, rue Bernard Gregory, Sophia Antipolis, F-06560 Valbonne, France*
(Received 3 August 2006; published 17 January 2007)

We calculate the energy of quantified levels in InGaAsN/AlGaAs quantum wells by using an analytical model based on the band anticrossing model and the repulsion by the nitrogen level. We show that the presence of nitrogen in InGaAsN quantum wells introduces peculiarities in the band structure. In quantum wells with a low confinement, energy levels are simply pushed towards the bottom of the well. When the confinement becomes large enough to support subbands above the localized nitrogen level, subbands are split and have a dispersion strongly affected by the repulsion by the *N* level. In this case, intersubband transitions are deeply modified, with a splitting of the transitions and important spectral shifts of the lines. Due to the admixing of nitrogen wave function in the electron wave function, the amplitude of the intersubband transitions decreases. The predicted effects are a clear test for the band anticrossing model on the one hand, and may have a strong impact on applications in the infrared on the other hand.

DOI: 10.1103/PhysRevB.75.045327 PACS number(s): 78.20.Bh, 71.20.Nr, 73.22.−f

## I. INTRODUCTION

The field of intersubband transitions (ISBT) was opened three decades ago in electron accumulation layers in silicon[1] and two decades ago in GaAs/AlGaAs quantum wells (QW).[2] Tremendous progress has been achieved from these early observations and has led to important applications including infrared imaging[3] and quantum cascade lasers.[4] In GaAs based heterostructures, the available spectral range is limited on the short wavelength side by the conduction band discontinuity to about 4 $\mu$m. Presently, only the AlGaN (Ref. 5) and InGaAs/AlAsSb (Ref. 6) material systems give rise to ISBTs at shorter wavelengths. In GaAs based materials, it has been proposed to use the InGaAsN alloy to reach wavelengths below 4 $\mu$m. The first observations of ISBT were made recently in InGaAsN/GaAs QWs.[7] The wavelength was however in the range of 10 $\mu$m due to the small confinement provided by GaAs barriers. In order to increase the confinement energy and decrease the ISBT wavelength, AlGaAs barriers are needed. The band offset which can be reached in InGaAsN/AlGaAs QWs can reach in theory almost 1 eV. In most materials, such a confinement would be large enough to support ISBT below 4 $\mu$m. In InGaAsN however, the structure of the conduction band is so peculiar that this point remains enigmatic. Two main descriptions of the GaAsN or InGaAsN conduction band have been proposed. The first one (band anticrossing or BAC model) is based on the repulsion between the $\Gamma$ point and the $N$ localized level[8–10] and accurately reproduces the observed dependence of the GaAsN or InGaAsN bandgap on the $N$ content.[11] The second approach is based on a pseudopotential supercell calculation of the band gap[12] and takes into account $N$ cluster states.[13] While these approaches largely differ, they both give similar results, at least for the conduction band minimum. In addition, the theoretical basis for using the BAC model was established from tight binding and extended *kp* calculations.[14] The following points have been noted in bulk InGaAsN and require a special attention when one wants to address ISBT and energy levels in InGaAsN QWs. First, the electron effective mass in the fundamental level (so called $E-$) is supposed to increase with $N$ content owing to the hybridization between the conduction band and a localized level. Second, not independent of the first point, the repulsion between the $N$ level and the conduction band introduces a nonparabolicity which increases with electron wave vector and prevents the $E-$ electron energy to get above the $N$ energy level. Third, there is an excited level (so called $E+$) above the $N$ level.

The purpose of this paper is to calculate the energy levels and the intersubband transitions in InGaAsN based heterostructures taking into account the aforementioned peculiarities of the diluted nitrides. In particular, we will address short wavelength ISBTs that involve energy levels close to or above the $N$ level.

## II. DERIVATION OF ANALYTICAL MODEL

As the band anticrossing model accurately describes the conduction band in InGaAsN and allows analytical calculations, we will use it. The $N$ level is located 1.65 eV above the valence band in GaAs, and this energy slightly increases with In content in InGaAs and depends on the local $N$ environment.[9,11] We use the repulsion potentiel parameters which best reproduce the experimental variation of InGaAsN band gap with In and N compositions.[11] In bulk InGaAsN, the BAC model predicts two levels given by[8]

$$E_+ = 0.5\left\{\left(E_N + E_\Gamma + \frac{\hbar^2 k^2}{2m^*_{\mathrm{InGaAs}}}\right) + \sqrt{\left(E_N - E_\Gamma - \frac{\hbar^2 k^2}{2m^*_{\mathrm{InGaAs}}}\right)^2 + 4V_N^2 x}\right\},$$

$$E_- = 0.5\left\{\left(E_N + E_\Gamma + \frac{\hbar^2 k^2}{2m^*_{\mathrm{InGaAs}}}\right) - \sqrt{\left(E_N - E_\Gamma - \frac{\hbar^2 k^2}{2m^*_{\mathrm{InGaAs}}}\right)^2 + 4V_N^2 x}\right\}, \quad (1)$$

where $V_N$ is the repulsion potential parameter and $x$ is the $N$

 ©2007 The American Physical Society

content. The lower level, $E-$, remains below the $N$ level $E_N$ while the upper level, $E+$ is above. These expressions of course do not apply for energy levels in QWs. It is however interesting to recall them in order to facilitate the discussion of the results that we obtain.

In InGaAsN QWs, we solve the Schödinger equation in the envelope function approximation by introducing the effective mass in InGaAs ($m^*_{\mathrm{InGaAs}}$) and the conduction band energy of strained InGaAs ($E_\Gamma$). The potential term includes the $N$ repulsion potential and the conduction band confinement energy. The envelope function approximation consists in separating the potential term in the initial Hamiltonian in two parts. The first one is the crystal potential which varies rapidly in space and the second is a potential which varies more slowly. The derivation of the BAC equation implicitly assumes that the $N$ potential varies more slowly than the crystal potential which allows to keep the $N$ potential and the confinement potential in the envelope function Hamiltonian while the crystal potential is described by the effective mass and the conduction band minimum.

We develop the wave function in the InGaAsN QW as a linear combination of a $\Gamma$ and $N$ functions, as is done in bulk InGaAsN

$$|\Psi\rangle = a|\Psi_\Gamma\rangle + b|\Psi_N\rangle,$$

$$|\Psi_\Gamma\rangle = (Ae^{ikz} + Be^{-ikz})u_c(r)e^{ik_{xy}r_{xy}}, \quad -L/2 < z < L/2,$$

$$|\Psi\rangle = Ce^{-\kappa(z-L/2)}u_c(r)e^{ik_{xy}r_{xy}}, \quad L/2 < z,$$

$$|\Psi\rangle = De^{\kappa(z+L/2)}u_c(r)e^{ik_{xy}r_{xy}}, \quad z < -L/2, \tag{2}$$

where $L$ is the QW width, $u_c$ is the Bloch function, $k_{xy}$ is the wave vector in the $xy$ plane that verifies the translational invariance in the plane. The $N$ wave function is unknown but we assume that it is localized and varies rapidly in space.

As in bulk material, we solve the Schrödinger equation by projection on the $\Gamma$ and $N$ functions and obtain the following Hamiltonian

$$\begin{vmatrix} \dfrac{\hbar^2k^2}{2m^*_{\mathrm{InGaAs}}} + \dfrac{\hbar^2{k_{xy}}^2}{2m^*_{\mathrm{InGaAs}}} - E & V_N * \sqrt{x} \\ V_N\sqrt{x} & E_N - E \end{vmatrix}, \tag{3}$$

which gives the dispersion of the $z$ wave vector in the InGaAsN QW

$$k = \sqrt{\frac{2m^*_{\mathrm{InGaAs}}}{\hbar^2}\left(E - \frac{\hbar^2{k_{xy}}^2}{2m^*_{\mathrm{InGaAs}}} + \frac{V_N^2}{E_N - E}\right)} \tag{4}$$

In the barrier we obtain as usual:

$$\kappa = \sqrt{\frac{2m_B}{\hbar^2}\left(V_B - E + \frac{\hbar^2{k_{xy}}^2}{2m_B}\right)}. \tag{5}$$

It is a common practice in GaAs/AlGaAs QWs (where $V_N = 0$) to take the same mass in the QW and in the barrier which allows to completely decouple the confinement energy and the kinetic energy in the $xy$ plane, leading to strictly parallel subbands. The error made by such an approximation

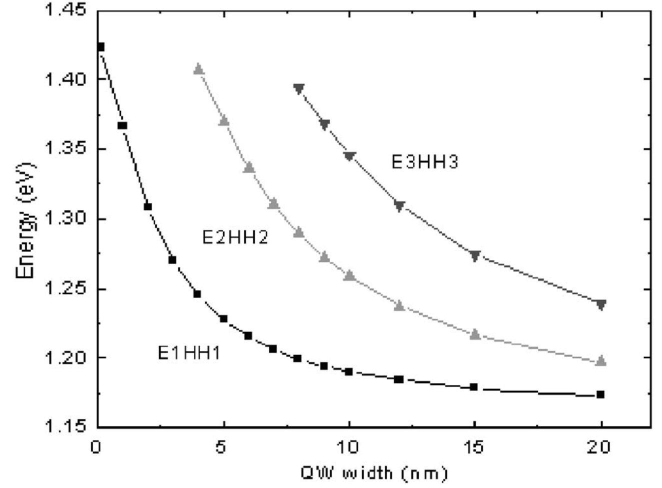


FIG. 1. Calculated transition energies in GaAsN/GaAs QWs as a function of well width. $N$ content=1.8%.

turns out to be in general negligible. Such decoupling between confinement energy and kinetic energy is absolutely impossible here due to the $V_N$ term (the uniform mass approximation will also not be used as it does not simplify the problem anymore). Hence, the energy level resolution has to be made for each value of the wave vector in the $xy$ plane. As a consequence, we can anticipate that electron subbands will be strongly nonparallel to each other.

The calculation then proceeds as usual, exploiting the continuity of the wave function and its derivative at the QW/barrier interfaces. As the $N$ function is supposed to vary rapidly in space, only the $\Gamma$ functions are considered to write the wave function continuity. Such a similar calculation and the same remark concerning the discontinuity of the $N$ wave function have been made by Tomić *et al.*[15] who, however, introduced a $N$ function in the barrier (with a null interaction) to ensure the wave function matching across the interface.

The calculation and the parameters that we used were first checked by calculating the interband transitions ($E_1HH_1$ and $E_2HH_2$) in many InGaAsN/GaAs QWs grown at the laboratory by molecular beam epitaxy where such transitions are easily observed in transmission. All calculations presented in this paper were done at 300 K. The agreement was very good but only QWs with low confinement were available. The second check was to compare with a full ten-band $kp$ model.[15] The agreement is excellent as can be seen by comparing our Figs. 1 and 5 of the latter paper.[15] The latter authors noted the same agreement between the $kp$ model and their analytical model. The pertinence of the BAC model for calculating the effective mass and the confinement energies has been confirmed.[16] We also compared our results with those obtained in 6 band, 8 band, and 10 band models.[17] Our value for the $E_1E_2$ transition in InGaAsN/GaAs QWs lies in between the values calculated with 10, 8, or 6 bands, indicating that our simple approach is not a priori inadequate. Again, the check was done for energies below the $N$ level (in that case, all subbands are below the $N$ level and the $N$ interaction simply pushes them towards lower energy) while we will also apply it to energies above the $N$ level. It is likely

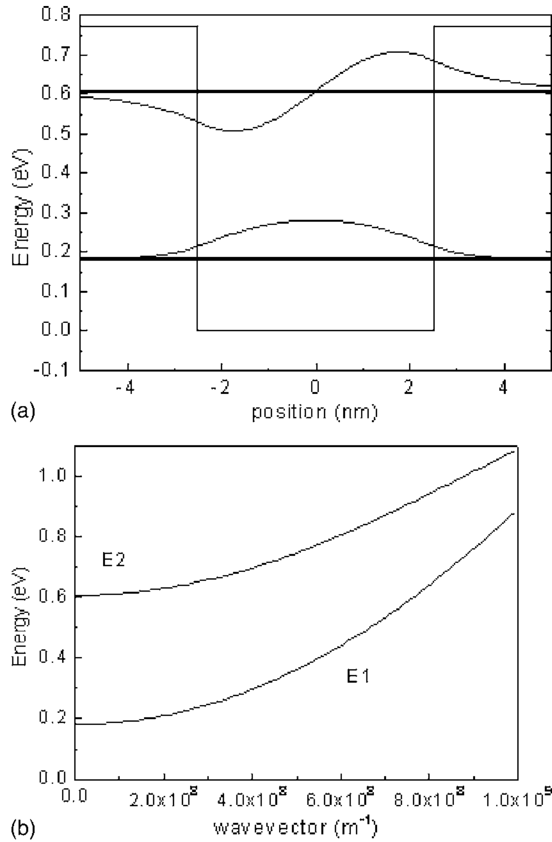


FIG. 2. Energy levels in an InGaAsN/AlGaAs QW (a) and dispersion of the subbands (b) in the *xy* plane. [In]=35%, [N]=0%, and [Al]=60%.

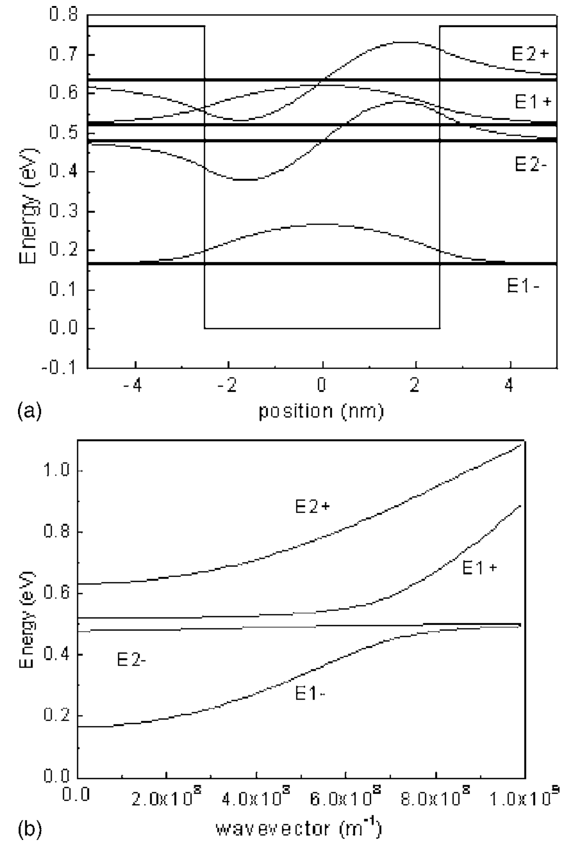


FIG. 3. Energy levels in an InGaAsN/AlGaAs QW (a) and dispersion of the subbands (b) in the *xy* plane. [In]=35%, [N]=0.1%, and [Al]=60%.

that the accuracy of the calculation degrades at higher energies. In particular, a 4 band BAC model involving the $X$ and $L$ conduction band levels[18] is likely to improve the accuracy at high energy. However, this would introduce additional parameters which are not precisely known and would introduce some arbitrary choices. We are confident that our simple model allows to point out the general trends and the main ideas.

### III. INTERSUBBAND TRANSITIONS

We now calculate the energy levels in QWs with a large confinement energy and the ISBT energies. The examination of the equation shows that no solution exists between the $N$ level and the $E_+$ energy [value calculated in the bulk by Eq. (1)]. As an example, we take an InGaAsN QW with 35% In, a width of 5 nm, and AlGaAs barriers with 60% Al. The bandgap of AlGaAs is indirect for Al contents above 40%. However, the band offset that must be used to calculate the confinement energies is the one related to the Γ level which increases with the Al content even above 40%. Figure 2(a) shows the energy levels for 0% $N$. There are two levels, one even and one odd level. Figure 2(b) shows the dispersion in the plane. Subbands are reasonably (not completely however as the uniform mass approximation is not used) parallel to each other, at least for small wave vectors.

We now increase the $N$ content to 0.1%. Figure 3 shows the energy levels and dispersion. We observe that the fundamental level is now split in two levels, with the same even symmetry (note that we show the Γ part of the wave function only, while the whole wave function also includes a $N$ function which allows for the orthogonality between levels). One is below $E_N$ and corresponds to the original fundamental level. It is built on the $E_-$ bulk level and can be called $E_{1-}$. The second is above $E_N$ and is a new feature, built on the $E_+$ level ($E_{1+}$). The dispersion allows to better understand the situation. These two levels result from the anticrossing with the $N$ level which occurs for $k \approx 7 \times 10^8$ m$^{-1}$. The first excited level is also split, with the difference that the new level ($E_{2-}$) is now below $E_N$ while the original one ($E_{2+}$) is above $E_N$. As a result of the anticrossing, the original fundamental level is pushed towards smaller energies while the original first level is pushed towards higher energies. Hence, the ISBT energy $E_1E_2$ (more precisely $E_{1-}E_{2+}$) is increased by the $N$ repulsion. It is important to stress that this conclusion is valid only for QWs with a high confinement where the first excited level is originally above $E_N$. In QWs with a low confinement, both the fundamental and the first excited levels are below $E_N$ and the $N$ repulsion tends to decrease the ISBT energy. In QWs with a high confinement, the $N$ repulsion helps to reach shorter ISBT wavelengths which is a positive effect for applications. However, the anticrossing splits the transition and reduces the oscillator strength for the

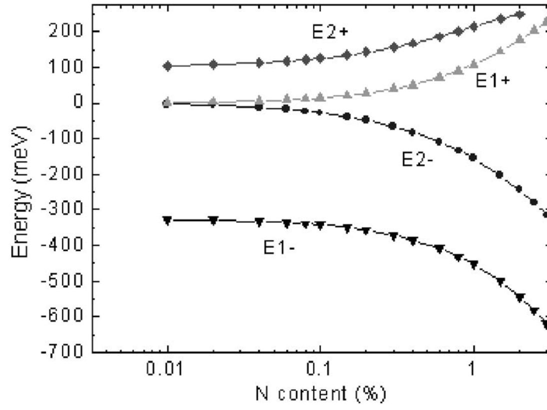


FIG. 4. Level energy versus $N$ content in an InGaAsN QW with 35% In, with $Al_{0.6}Ga_{0.4}As$ barriers. Energy is calculated relative to the energy of the $N$ level.

high energy transition. A second transition appears between the fundamental and the split $E_2$ level ($E_{1-}E_{2-}$). Other ISBTs such as $E_{1+}E_{2-}$ or $E_{1+}E_{2+}$ exist but are not considered here for absorption as only the fundamental is populated with electrons in normal conditions. It is interesting to note that such a dispersion has been experimentally (with some differences due to differences in the parameters of the structure) observed by magneto-transport in a resonant tunneling diode by Patane *et al.*[19]

Figure 4 shows the variation of the level energies with the $N$ content. For clarity, energies are shown relative the $N$ level. The increasing repulsion from the $N$ level is clearly seen. At 0% $N$, only levels $E_1$ and $E_2$ exist at −325 and 101 meV. With increasing $N$ content, levels emerge with an increasing energy separation from the $N$ level. At 0% $N$, only one ISBT exist at 426 meV ($E_{1-}E_{2+}$). With increasing $N$ content, this energy increases while a second transition ($E_{1-}E_{2-}$) appears at 325 meV and then shifts towards lower energies.

In order to better appreciate the effect of $N$ introduction on the intensity of the transitions we now calculate the ISBT oscillator strength. The analysis is restricted here to the case of absorption from the fundamental level to the $n$ excited state (case for detectors for instance). The amplitude of the ISBT is calculated from the dipolar interaction

$$\text{Amplitude} \propto (a_1\langle\Psi_\Gamma 1| + b_1\langle\Psi_N|)e\mathbf{E}\cdot\mathbf{r}(a_n|\Psi_\Gamma n\rangle + b_n|\Psi_N\rangle)^2. \tag{6}$$

The amplitude is proportional to the square of the dipole element $d$, which is given by

$$d = (a_1\langle\Psi_\Gamma 1| + b_1\langle\Psi_N|)z(a_n|\Psi_\Gamma n\rangle + b_n|\Psi_N\rangle),$$

$$d = a_1^* a_n\langle\Psi_\Gamma 1|z|\Psi_\Gamma n\rangle + a_1^* b_n\langle\Psi_\Gamma 1|z|\Psi_N\rangle + b_1^* a_n\langle\Psi_N|z|\Psi_\Gamma n\rangle + b_1^* b_n\langle\Psi_N|z|\Psi_N\rangle. \tag{7}$$

The first term is the usual term multiplied by $a_1{}^* a_n$. This is an important point. The ISBT amplitude is reduced by the fact that the wave function is not a pure Γ function anymore and contains some $N$ function. The second and third terms are negligible as the $N$ function is rapidly varying in space (much more than the envelope function) so that the integral vanishes. The fourth term is null by symmetry. Before giving numerical illustrations, we can anticipate that the $N$ part in the wave function increases when the energy gets closer to the $N$ level. In Fig. 3 for instance, this is the case for $k < 7 \times 10^8\ \text{m}^{-1}$ for the $E_{1+}$ subband, for $k > 7\times 10^8\ \text{m}^{-1}$ for the $E_{1-}$ subband, and for any k for the $E_{2-}$ subband. In other words, IST will remain strong for subbands far away from the $N$ level, with a (quasi) parabolic dispersion and thus reasonably parallel to each other. A similar remark has been done for the magnetotransport in a resonant tunnel diode by Endicott *et al.*[20] The tunnel probability between GaAs Γ states and the resonant InGaAsN level depends on the Γ part of the electron wave function in the QW. The nature of the electron wave function in InGaAsN QWs is thus a crucial issue for many aspects of physics, and we show that ISBTs are very sensitive to this point. The Γ part of the wave function is the a coefficient which can be easily calculated

$$a = \frac{(E - E_N)}{V_N} b = \frac{(E - E_N)}{\sqrt{V_N^2 + (E - E_N)^2}}. \tag{8}$$

Equation (8) explicitly shows that the Γ part decreases with the energy separation from the $N$ level. Note that this coefficient has to be calculated for each value of the in plane wave vector. The $\langle\Psi_\Gamma 1|z|\Psi_\Gamma n\rangle$ term also has to be calculated for each value of the in plane wave vector. In order to calculate the absorption, we partially fill the fundamental subband with electrons ($n$ doping) up to the Fermi wave vector. The absorption is then calculated by integrating up to the Fermi wave vector all transitions from the fundamental to the upper levels, each transition having an amplitude given by Eqs. (6)–(8). In order to account for the finite lifetime of excited levels and the related homogeneous broadening, the spectrum is convoluted with a Lorentzian function with a broadening parameter $\Gamma = \sqrt{(kT)^2 + (\frac{2\hbar}{T_2})^2}$, where the coherence time $T_2$ has been taken to be equal to 0.15 ps, which is the typical value in GaAs based QWs, and where a thermal broadening has been added.

We present now some ISBT spectra calculated by our model. We have chosen an InGaAsN QW with GaAs spacers and AlGaAs barriers. GaAs spacers are inserted as it is preferable from the growth point of view to avoid an InGaAsN/AlGaAs interface because of possible AlN bonds that could form[21] and degrade the crystallographic quality of the sample. Although this paper deals with calculations only, we prefer to present structures that can realistically be grown, which we hope will trigger some experimental work. The In content is 40%, the $N$ content is 1% and the Al content is 40%. The spacer is 1 nm thick and the QW is 2.5 nm thick. Two separate absorption peaks are visible in the spectrum shown in Fig. 5 at about 0.3 and 0.47 eV. Let us mention that the same QW without $N$ exhibits a single absorption peak at about 0.35 eV. When the doping increases, the intensity of both peaks increases first almost linearly up to a density of about $10^{12}\text{-cm}^{-2}$. Then the low energy peak saturates while the high energy peak keeps growing. This effect is due to the difference in dispersion of the two subbands that support the ISBTs. The low energy transition is based on $E_{2-}$

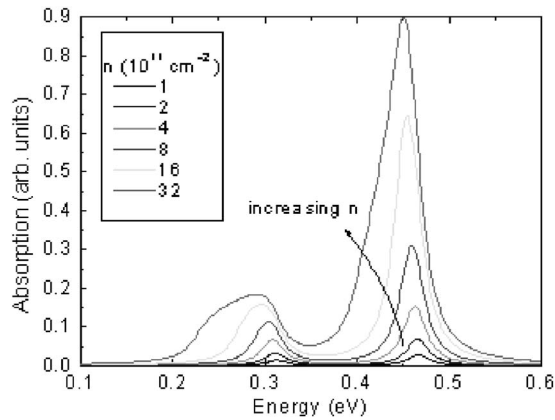


FIG. 5. Theoretical absorption spectra at 300 K in InGaAsN/GaAs/AlGaAs QWs for increasing electron densities: 1, 2, 4, 8, 16, and $32 \times 10^{11}$ cm$^{-2}$. QW thickness=2.5 nm. GaAs spacer=1 nm. [In]=40%, [N]=1%, and [Al]=40%.

while the high energy one is based on $E_{2+}$. At low electron densities, only small $k$ states in the fundamental subband are populated and both transitions involve $E_2$ final states which contain little $N$ wave function so that the ISBT is large and increases with doping. At large densities however, large $k$ states are involved. As $E_{2-}$ states become $N$ rich, the corresponding transitions become weak and the absorption saturates. On the contrary $E_{2+}$ states contain less and less $N$ and thus have a large oscillator strength, so that the absorption increases with doping. Such a strong dependence of the absorption spectrum on the doping is a peculiar behavior due to the effect of $N$ on the band structure.

We now discuss the effect of $N$ on the intensity of the ISBT. The effect strongly depends on the QW structure. In the previous structure (Fig. 5) the absorption amplitude at 0.47 eV (1% $N$) is smaller than the one at 0.35 eV (0% $N$) by a factor of 10. In other cases, the reduction in ISBT amplitude is much smaller. Figure 6 presents the absorption spectrum in an InGaAsN/GaAs/AlGaAs Qw as a function of $N$ content. The QW width is 2 nm, the spacer is 0.5 nm thick, the In and Al contents are 40% and 80%, respectively. This structure was chosen so as to push the $E_{2-}$ closer to the $N$ level in order to reduce its oscillator strength while pushing the $E_{2+}$ far away above the $N$ level in order to increase its oscillator strength. When the $N$ composition increases from 0 to 1%, the amplitude of the ISBT decreases from 0.98 to 0.37 (arbitrary units), which is a factor 2.6. Correlatively, the low energy transition remains negligible (the amplitude of the peak at 0.2 eV is about 0.005 for 1% $N$). In the same time, the transition energy shifts from 0.51 to 0.67 eV which is a strong effect.

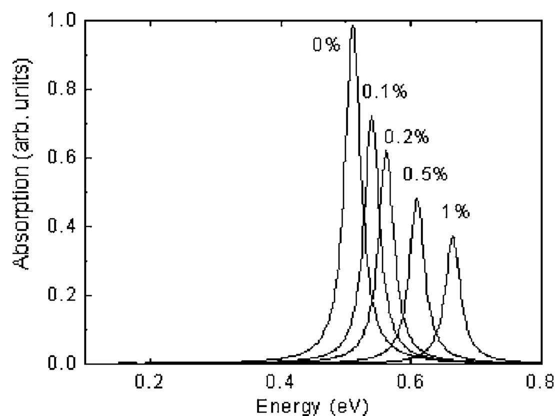


FIG. 6. Theoretical absorption spectra in InGaAsN/GaAs/AlGaAs QWs for increasing $N$ compositions (0, 0.1, 0.2, 0.5, and 1%). [Al]=80% and [In]=40%. GaAs spacer =0.5 nm. QW thickness=2 nm. Electron density=$5 \times 10^{11}$ cm$^{-2}$.

We have discussed so far the splitting of ISBTs due to the introduction of $N$ for high confinement QWs. The splitting of band to band transitions such as the $E_2HH_2$ transition is also predicted and should be easier to observe than the splitting of ISBTs. Indeed, ISBTs are weaker and generally broader than band to band transitions. Experimentally, band to band transitions are observed in many samples with various structures, while ISBTs have been observed so far in a limited number of samples (and in particular only samples with low confinement QWs). One difficulty in the observation of the splitting of band to band transition in QWs with a high confinement arises from the energy of the transition which is larger than the GaAs band gap energy, preventing all measurements by transmission and making measurements by reflection difficult. Back etching the substrate should in principle allow such measurements to be performed.

As far as applications are concerned, we have seen that with a reasonable Al content in the barrier (40%, corresponding to Fig. 5), the introduction of $N$ allows us to shift the ISBT wavelength from 3.5 $\mu$m to 2.65 $\mu$m. In practice, it has been observed that In segregation in the QW tends to increase the transition wavelength. With this correction in mind, we can claim that the introduction of $N$ in such structures should allow us to shift the wavelength from 4 to 3.2 $\mu$m, which is a decisive bonus for infrared imagers based on ISBT in the 3–5 window. The decrease of the ISBT amplitude can be minimized compared to the one presented here by a proper design of the QW, but cannot be suppressed. Some compromise can probably be found between the spectral shift and the decrease of oscillator strength so that we are confident that InGaAsN can be advantageously used for infrared imagers based on ISBTs.

A specific issue concerning ISBT is the polarization selection rule. In the present simple model, the ISBTs are related to $\Gamma$ subbands only [Eqs. (6) and (7)] so that the same selection rules are predicted for InGaAsN QWs as for InGaAs QWs. At first approximation, the TM polarization selection rule applies i.e. only photons with some vertical (along the growth axis) component of the electric field can induce ISBTs. It has been claimed that this selection rule could be violated in GaAs or InGaAs QWs.[22] While very little evidence was found to support such an assertion in GaAs QWs, it can be accepted that the mixing of the conduction and valence bands increases when the band gap energy decreases which should lead to a partial violation of the selection rule. As the band gap in InGaAsN is much smaller than in GaAs for instance, one could expect the selection rule not to be strictly obeyed. A full calculation with valence and conduction bands should in principle answer the question. An interesting issue would then be to determine the effect of N wave

function in the violation of the selection rule, if any.

Finally, we would like to comment on issues related to the BAC model used here and its limits. Nitrogen clusters are not taken into account in the BAC model, while they introduce resonant energy levels within the conduction band.[13] Magnetotransport in a resonant tunneling diode by Patane *et al.*[19] support the presence of such levels. As far as ISBTs are concerned, such levels could couple with the subbands and split them (for instance considering one cluster level, in addition to the isolated *N* level, would lead to triple subbands, and triple ISBTs). However, these levels are in general close to the *N* level, close together, and in quite a large number. Hence it is not clear whether the splitting with these cluster levels could be observed. It is likely that the main effect would be to broaden the main two lines that were calculated in this paper. Experimental data on this point, provided the resolution is good enough, would clearly allow us to test the limits of the BAC model.

## IV. CONCLUSION

We have shown that the presence of *N* in InGaAsN QWs introduces peculiarities in the band structure. In QWs with a low confinement, energy levels are simply pushed towards the bottom of the well. In QWs with a large confinement, subbands are split and have a dispersion strongly affected by the repulsion by the *N* level. In this case, ISBTs are deeply modified, with a splitting of the transitions and important spectral shifts of the lines. Due to the admixing of *N* wave function in the electron wave function, the amplitude of the ISBT decreases. However, by a proper design of the QW, this effect can be minimized and the new spectral domain (wavelength below 4 $\mu$m) that is permitted by the introduction of *N* makes InGaAsN a promising candidate for infrared applications. From the fundamental point of view, the study of ISBTs at high energy and the observation of the effects predicted in this paper would be a clear and decisive test of validity of the band anticrossing model.

## ACKNOWLEDGMENTS

This work is partly supported by the ACI-BAND project (NR0025). Fruitful discussions with Borge Vinter and Bernard Gil are acknowledged.

*Electronic address: jyd@crhea.cnrs.fr

[1] A. Kamgar, P. Kneschaurek, G. Dorda, and J. F. Koch, Phys. Rev. Lett. **32**, 1251 (1974).
[2] L. C. West and S. J. Eglash, Appl. Phys. Lett. **46**, 1156 (1985).
[3] B. F. Levine, J. Appl. Phys. **74**, R1 (1993); *Proceedings of SPIE Volume: 5783, Infrared Technology and Applications XXXI*, edited by B. F. Andresen and G. F. Fulop, ISBN 0-8194-5768-X (2005).
[4] J. Faist, F. Capasso, D. L. Sivco, C. Sirtri, A. L. Hutchinson, and A. Y. Cho, Science **264**, 553 (1994); C. Sirtori and J. Nagle, C. R. Phys. **4**, 639 (2003).
[5] C. Gmachl, H. M. Ng, and A. Y. Cho, Appl. Phys. Lett. **79**, 1590 (2001); C. Gmachl, H. M. Ng, S.-N. G. Chu, and A. Y. Cho, *ibid.* **77**, 3722 (2000).
[6] T. Mozume, H. Yoshida, A. Neogi, and M. Kudo, Jpn. J. Appl. Phys., Part 1 **38**(2B), 1286 (1999); A. Neogi, T. Mozume, H. Yoshida, and O. Wada, IEEE Photon. Technol. Lett. **11**, 632 (1999).
[7] J. Y. Duboz, J. Gupta, M. Byloss, H. C. Liu, and Z. Wasilewski, Appl. Phys. Lett. **81**, 1836 (2002).
[8] W. Shan, W. Walukiewicz, J. W. Ager III, E. E. Haller, J. F. Geisz, D. J. Friedman, J. M. Olson, and S. R. Kurtz, Phys. Rev. Lett. **82**, 1221 (1999).
[9] P. J. Klar, H. Grüning, J. Koch, S. Schäfer, K. Volz, W. Stolz, W. Heimbrodt, A. M. Kamal Saadi, A. Lindsay, and E. P. O'Reilly, Phys. Rev. B **64**, 121203(R) (2001).
[10] A. Lindsay and E. P. O'Reilly, Solid State Commun. **112**, 443 (1999).
[11] J.-Y. Duboz, J. A. Gupta, Z. R. Wasilewski, J. Ramsey, R. L. Williams, G. C. Aers, B. J. Riel, and G. I. Sproule, Phys. Rev. B **66**, 085313 (2002).
[12] E. D. Jones, N. A. Modine, A. A. Allerman, S. R. Kurtz, A. F. Wright, S. T. Tozer, and X. Wei, Phys. Rev. B **60**, 4430 (1999); T. Mattila, S. H. Wei, and A. Zunger, *ibid.* **60**, R11245 (1999); P. R. C. Kent and A. Zunger, Phys. Rev. Lett. **86**, 2613 (2001); Y. Zhang, A. Mascarenhas, H. P. Xin, and C. W. Tu, Phys. Rev. B **63**, 161303 (2001).
[13] P. R. C. Kent and A. Zunger, Phys. Rev. B **64**, 115208 (2001).
[14] E. P. O'Reilly, A. Lindsay, S. Tomić, and M. Kamal-Saadi, Semicond. Sci. Technol. **17**, 870 (2002).
[15] S. Tomić, E. P. O'Reilly, P. J. Klar, H. Grüning, W. Heimbrodt, W. M. Chen, and I. A. Buyanova, Phys. Rev. B **69**, 245305 (2004).
[16] S. Tomić and E. P. O'Reilly, Phys. Rev. B **71**, 233301 (2005).
[17] S. T. Ng, W. J. Fan, Y. X. Dang, and S. F. Yoon, Phys. Rev. B **72**, 115341 (2005).
[18] B. Gil, Solid State Commun. **114**, 623 (2000).
[19] A. Patane, J. Endicott, J. Ibanez, P. N. Brunkov, L. Eaves, S. B. Healy, A. Lindsay, E. P. O'Reilly, and M. Hopkinson, Phys. Rev. B **71**, 195307 (2005).
[20] J. Endicott, A. Patane, J. Ibanez, L. Eaves, M. Bissiri, M. Hopkinson, R. Airey, and G. Hill, Phys. Rev. Lett. **91**, 126802 (2003).
[21] I. P. Vorona, T. Mchedlidze, D. Dagnelund, I. A. Buyanova, W. M. Chen, and K. Köhler, Phys. Rev. B **73**, 125204 (2006).
[22] L. H. Peng, J. H. Smet, T. P. E. Broekaert, and C. G. Fonstad, Appl. Phys. Lett. **61**, 2078 (1992).